Advanced Composite Materials
Publication details, including instructions for authors and subscription information:
http://www.tandfonline.com/loi/tacm20

Prediction of creep rupture in unidirectional composite: Creep rupture model with interfacial debonding and its propagation

Jun Koyanagi , Genya Kiyota , Takashi Kamiya & Hiroyuki Kawada

Version of record first published: 02 Apr 2012.

To cite this article: Jun Koyanagi , Genya Kiyota , Takashi Kamiya & Hiroyuki Kawada (2004): Prediction of creep rupture in unidirectional composite: Creep rupture model with interfacial debonding and its propagation, Advanced Composite Materials, 13:3-4, 199-213

To link to this article: http://dx.doi.org/10.1163/1568551042580190

Adv. Composite Mater., Vol. 13, No. 3-4, pp. 199–213 (2004)

Also available online - www.vsppub.com

Prediction of creep rupture in unidirectional composite: Creep rupture model with interfacial debonding and its propagation

JUN KOYANAGI [1,*], GENYA KIYOTA [1], TAKASHI KAMIYA [1] and HIROYUKI KAWADA [2]

[1] *Graduate School of Waseda University, 3-4-1 Okubo, Shinjuku, Tokyo, 169-8555, Japan*
[2] *Department of Mechanical Engineering, Waseda University, 3-4-1 Okubo, Shinjuku, Tokyo, 169-8555, Japan*

Received 19 December 2003; accepted 6 April 2004

Abstract—This paper describes a creep rupture model that takes into account the interfacial debonding and its propagation around broken fibers in unidirectional fiber-reinforced polymers. The interfacial debonding is accompanied by fiber breaks under a longitudinal tensile load, and the interfacial debonding length depends on both the fiber stress at the moment of the fiber breaks and the properties of the interfacial adhesion. In this paper, the interfacial debonding length, its propagation as a function of time, the probability of fiber breaks and an interfacial shear stress are investigated by fragmentation tests with a single glass fiber embedded in each vinylester resin specimen. Subsequently, it was found that a relationship between the fiber strength and the fiber effective length, the length of the debonding length and stress recovery length subtracted from one fiber length, was log linear, and that the larger the fiber stress, the longer was the interfacial debonding length. Next, creep tests were performed to investigate the creep constants of the vinylester resin, and interfacial debonding propagation tests were also performed to identify the interfacial debonding-propagation behavior as a function of time using single fiber composites subjected to constant strains. We modified the creep rupture model by taking into account the interfacial debonding length, which has a time-dependent characteristic, into a conventional Curtin–McLean creep rupture model. It was found that the predicted creep rupture time of the modified model was shorter than that of the conventional model and that there was no threshold creep stress in the modified model unlike in the conventional model because the interfacial debonding propagation makes the prediction creep rupture time lower as time progresses.

Keywords: Interfacial debonding; creep rupture; unidirectional composite.

*To whom correspondence should be addressed. E-mail: jun@kawada.mech.waseda.ac.jp

1. INTRODUCTION

Due to the increasing number of applications for advanced polymer matrix composites in engineering structures, we need to be able to predict their reliability during long-term service. Their long durability under tensile stress is one of the most critical concerns because composites do not fail instantaneously but undergo long-term creep. It is a well-known fact that composites exhibit transient and steady state creep stages and eventually they fail by creep rupture, as with metallic materials. Similarities found in most composite creep studies are that time-to-failure is statistical and fiber breaks occur throughout the composite lifetime, being especially intense upon initial loading and at the time of creep rupture.

McLean [1] described the creep behavior of unidirectional composites. It was assumed that a fiber was elastic and a matrix was viscoelastic. The matrix stress transfers stress to the fiber as time progresses and causes an increase in the fiber strain to equal the composite strain. Curtin [2] estimated the rupture strain and the maximum fiber stress of unidirectional composites in order to estimate the probability of breakage of the fiber in its own cross-section. Additionally, Du and McMeeking [3–5] predicted the creep rupture time of unidirectional composites under tensile loads. They considered that the strain (stress) of the McLean model had reached the rupture of that of the Curtin model. But this creep rupture model had overestimated the creep rupture time in comparison with actual experiments. Some of the contributing factors of this phenomenon are the stress concentration on the adjacent fibers, the increasing of the stress recovery length and the occurrence of interfacial debonding. Clearly, such complexities are undetectable on a macroscopic scale, and thus, we took the micro-mechanical behavior, specifically the interfacial debonding, into account for our creep rupture model.

Wagner and co-workers [6–8] investigated the interfacial debonding length around the fiber breaks of the single fiber within polymer matrix specimen in fragmentation tests. The interfacial debonding energy was taken as an interfacial property and was used in the search for fracture criteria as an energy-based theory. Generally, the interfacial shear stress has been regarded as an interfacial property, but this is not suitable because interfacial shear stress depends on the shear direction properties of a matrix. To generalize the interfacial property, one should employ the interfacial debonding energy as a parameter of the interfacial fracture. In their study, the fragmentation tests were performed using single fiber composite specimen made of a single glass fiber within a dog-bone shape polymer. They confirmed that one could evaluate the interfacial property with the interfacial debonding length. Also, Beyerlein [9, 10] and co-workers evaluated a growth of the inelastic zone that could possibly be an interfacial debonding or plastic zone or anything. In this theory, the shear stress of the interface around the fiber breaks relaxes by means of the viscoelastic matrix and promotes a propagation of the interfacial debonding. This time-dependent failure process primarily begins with the effects of the matrix creep relaxation and goes on long-term creep. Therefore, we also have to identify the

propagation of the interfacial debonding for an assurance of the durability of the polymer matrix composite in a long-term creep life.

In this study, glass fiber/vinylester interfacial properties and the fiber strength as a function of the fiber length are investigated in fragmentation tests. The interfacial shear stress is calculated based on the Kelly-Tyson model by taking into account the interfacial debonding length at the critical fragment state. The fiber strength is also calculated in its own length without the interfacial debonding length and the stress recovery length. The propagation behavior of the interfacial debonding is investigated in constant strain tests using fragmentation specimen. To investigate the creep parameters, creep tests are performed by the use of unidirectional composites. The maximum failure strain of the modified Curtin model, which takes into account the interfacial debonding length of unidirectional composites, is estimated from these derived parameters. In this model, we assume that the interfacial shear stress on the interfacial debonding area is neglected, that is, the interfacial friction is neglected. This model calculates a lower failure strain than the conventional Curtin model, so it predicts that the creep rupture time is shorter and that there will be no threshold creep stress.

2. CONVENTIONAL CREEP MODELS

2.1. Creep behavior of unidirectional composite

McLean derived a creep strain behavior of a unidirectional composite as follows. He assumed that the fiber was elastic and the matrix was viscoelastic; therefore

$$\varepsilon = \sigma_f / E_f, \tag{1}$$

$$\dot{\varepsilon} = \dot{\sigma}_m / E_m + B\sigma_m^n, \tag{2}$$

where ε is the total strain, B, n is the creep coefficient, σ_f is the fiber stress, σ_m is the matrix stress, E_f is Young's modulus of the fiber, E_m is Young's modulus of the matrix and $(\dot{})$ denotes differentiation with respect to time.

Generally, the fiber stress and the matrix stress are important in a unidirectional composite as follows

$$\sigma = (1 - V_f)\sigma_m + V_f\sigma_f,$$

where V_f is the fiber volume fraction.

From these three equations, the total composite strain is derived as a function of time:

$$\varepsilon(t) = \frac{\sigma}{V_f E_f} - \frac{1 - V_f}{V_f E_f}\left\{\left(\frac{E_m\sigma}{E_c}\right)^{1-n} + \frac{(n-1)V_f E_f E_m B t}{E_c}\right\}^{1/(1-n)}, \tag{3}$$

$$E_c = (1 - V_f)E_m + V_f E_f, \tag{4}$$

where E_c is the Young's modulus of the entire unidirectional composite.

2.2. Curtin model

Curtin estimated the fracture strain and stress of unidirectional composites in order to consider the probability of fibers breaks occurring within a particular thickness in its cross-section. The interfacial shear stress was assumed constant in the area of the stress recovery length (L_f). Figure 1 shows a shear stress distribution of the interface around a broken fiber. As shown in Fig. 1, the average of fiber stress $\bar{\sigma}_f$ is

$$\bar{\sigma}_f = (1-q)E_f\varepsilon + \frac{qE_f\varepsilon}{2}. \tag{5}$$

Here q is the probability of fiber breaks in the $2L_f$ length. Generally, the fiber breaks probability is as follows, using Weibull parameters L_0, m and σ_0.

$$P = 1 - \exp\left(-\frac{L}{L_0}\left(\frac{\sigma}{\sigma_0}\right)^m\right). \tag{6}$$

The probability of fiber breaks q in the $2L_f$ length is

$$q = 1 - \exp\left(-\frac{2L_f}{L_0}\left(\frac{E_f\varepsilon}{\sigma_0}\right)^m\right). \tag{7}$$

Here, the fiber stress σ can be substituted with $E_f\varepsilon$ because the fiber is assumed to be elastic. This equation can also be expressed as follows:

$$\ln(1-q) = -\frac{2L_f}{L_0}\left(\frac{E_f\varepsilon}{\sigma_0}\right)^m. \tag{8}$$

When q is small, equation (8) can be expressed approximately as follows:

$$q = (2L_f/L_0)(E_f\varepsilon/\sigma_0)^m. \tag{9}$$

From an interfacial force balance equation based on a shear lag theory, L_f can be derived as follows:

$$L_f = E_f\varepsilon D/4\tau_0, \tag{10}$$

where D is the fiber diameter, and τ_0 is the interfacial shear stress.

The fiber breaks probability equation (9) is described using characteristic stress S_c and strain as shown in equation (11).

$$q = \left(\frac{E_f\varepsilon}{S_c}\right)^{m+1}, \tag{11}$$

$$S_c = \left(\frac{2\sigma_0^m\tau_0L_0}{D}\right)^{1/(m+1)}. \tag{12}$$

Thus, the average of the fiber stress is

$$\bar{\sigma}_f = E_f\varepsilon\left\{1 - \frac{1}{2}\left(\frac{E_f\varepsilon}{S_c}\right)^{m+1}\right\}. \tag{13}$$

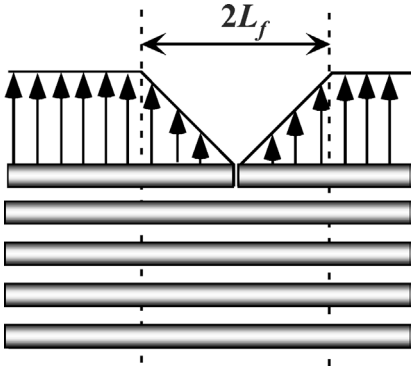

Figure 1. Schematic of fiber stress distribution around the fiber break in its own cross-section.

A differential equation of equation (13) can calculate the maximum stress of the average fiber stress by assuming that the differential coefficient is 0; and the strain in which the differential coefficient is equal to 0 can also be calculated. The maximum value of the fiber stress average is the fracture stress and the strain at that stress is the rupture strain of the unidirectional composites. These are as follows:

$$S_{\max} = S_c \frac{m+1}{m+2}\left(\frac{2}{m+2}\right)^{1/(m+1)}, \tag{14}$$

$$\varepsilon = \frac{S_c}{E_f}\left(\frac{2}{m+2}\right)^{1/(m+1)}. \tag{15}$$

This means that when the stress or the strain reaches these values, unidirectional composites fail at static loading conditions.

2.3. Creep rupture model

Du and McMeeking predicted the creep rupture time in unidirectional composites under tensile loads. They assumed that when the composite strain (or stress) of the McLean model had reached the rupture strain (or stress) of the Curtin model, the composite would fail: they verified this behavior from experimental results and numerical analyses. It was found that the creep rupture time could be predicted by substituting the rupture strain of the Curtin model with the strain of the McLean model. The creep rupture time can be expressed as the following equation:

$$t_r = \frac{E_c}{(n-1)V_f E_f E_m B}\left[\left(\frac{1-V_f}{\sigma - V_f S_{\max}}\right)^{n-1} - \left(\frac{E_c}{E_m \sigma}\right)^{n-1}\right]. \tag{16}$$

Thus far, it is possible to predict the creep rupture time that is caused by the accumulation of micro-damage (fiber breaks) in unidirectional composites. This creep rupture model is called the Curtin–McLean model.

3. PROPOSED CREEP RUPTURE MODEL

It is well known that there are several kinds of micro-damage in composites. Interfacial debonding and fiber breaks are some typical examples. In the above Curtin model, the probability of fiber breaks was taken into account, but interfacial debonding was ignored. Interfacial debonding can be a disastrous kind of damage in cases where the interfacial property is weak. We assume that interfacial debonding needs to be taken into account in the creep rupture model. Because the interfacial debonding could propagate as time progresses, it might become the fatal damage for the composite even if the interfacial property was strong.

First of all, we assume the stress distribution is around the broken fibers. Figure 2 shows the fiber stress distribution around the broken fibers. It is assumed that the interfacial frictional shear stress is neglected in the interfacial debonding region.

This stress distribution is applied to the Curtin model. The thickness of the cross-section of the Curtin model changes from $2L_f$ to $2L_f + L_d(t)$ as shown in

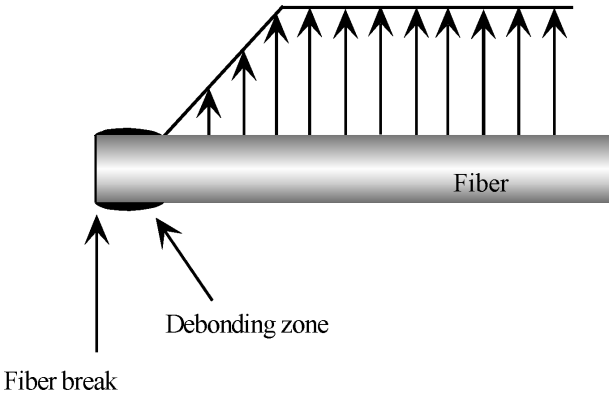

Figure 2. Tensile stress distribution of fiber with interfacial debonding.

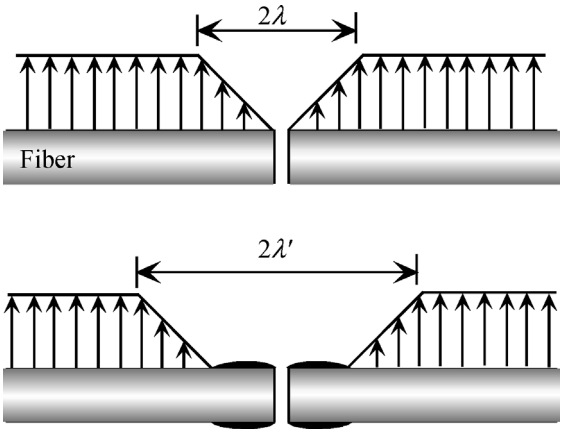

Figure 3. Stress recovery length with interfacial debonding.

Fig. 3. Here, $L_d(t)$ is the interfacial debonding length as a function of time. So the probability of fiber breaks and the average of the fiber stress must be estimated in the range of its own cross-section having a $2L_f + L_d(t)$ thickness. These are changed respectively as follows. The probability of the fiber breaks is

$$q = \left(\frac{2L_f + L_d}{L_0}\right)\left(\frac{E_f\varepsilon}{\sigma_0}\right)^m, \tag{17}$$

where $L_d(t)$ is the interfacial debonding length and the average of fiber stress is

$$\bar{\sigma}_f = (1-q)E_f\varepsilon + qE_f\varepsilon\frac{L}{2L_f + L_d}. \tag{18}$$

It is possible to estimate the rupture stress and strain taking into account the interfacial debonding length by using equations (17) and (18). The prediction of the creep rupture time is as follows by the use of the modified parameters mentioned above.

$$t_r = \frac{E_c}{(n-1)V_f E_f E_m B}\left[\left(\frac{1-V_f}{\sigma - V_f S'_{\max}}\right)^{n-1} - \left(\frac{E_c}{E_m\sigma}\right)^{n-1}\right], \tag{19}$$

where $S'_{\max}$ is the modified maximum fiber stress.

4. EXPERIMENTAL

4.1. Fragmentation test

Fragmentation tests were performed to investigate the initial interfacial debonding length, the relationship between the fiber length and the fiber strength, and the interfacial shear stress. Table 1 shows the mechanical properties of the fragmentation specimen, and Fig. 4 shows the specimen size and dimensions. The specimen is called a single fiber composite (SFC); the single fiber is a glass fiber and the matrix is a vinylester resin. We made an *in-situ* observation using a fragmentation test system that consisted of a small capacity tensile test machine (MINIMAT) on the stage of an optical microscope as shown in Fig. 5. The test results of the static fragmentation tests were as follows.

Firstly, Fig. 6 shows the initial interfacial debonding length in static fragmentation tests. Generally speaking, the more the fiber strain increases, the longer is the initial interfacial debonding length. In this study, we dealt with the interfacial debonding

Table 1.
Mechanical properties of specimen

Young's modulus of fiber	E_f	72 GPa
Fiber diameter	D	22.5 μm
Gage length	L_0	25 mm

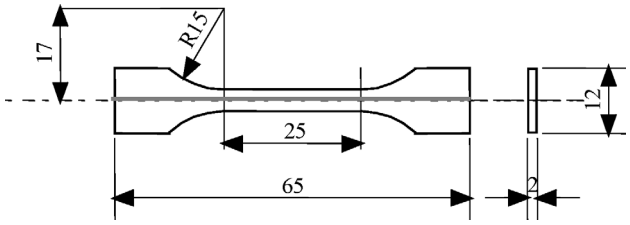

Figure 4. Dimensions of fragmentation's specimen.

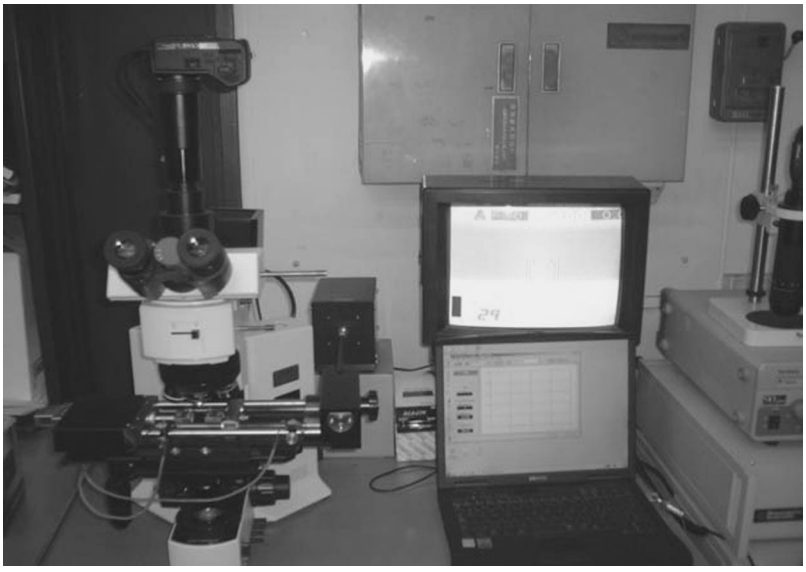

Figure 5. System of fragmentation tests.

length along with a quadric as a function of the strain. The glass fiber/vinylester interfacial debonding length can be expressed as

$$L_d = 11 \times \varepsilon^2 + 1.3 \times \varepsilon. \tag{20}$$

Secondly, the result of the fiber strength is indicated as follows. The relationship between the probability of the fiber breaks and the fiber length in the situation in which fibers are embedded in the matrix by fragmentation tests can be calculated from the relationship of the number of fragments and the specimen strain. Here, the fiber length is defined by dividing the total fiber length by the number of fiber breaks. This was the way it was evaluated conventionally. But this method is not available in those cases when stress recovery length or the interfacial debonding length are relatively long. Because the probability of fiber breaks is relatively lower in the stress recovery length or the interfacial debonding length due to the fact that the fiber stress is clearly smaller in these regions, to include these lengths into the fiber length would not be appropriate for the estimation of the fiber strength in such cases. To estimate the relationship of the fiber strength and the fiber length exactly,

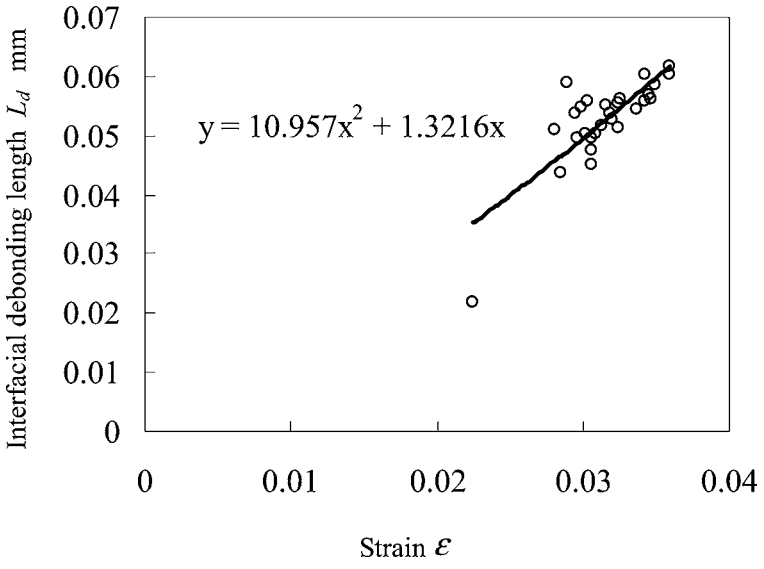

Figure 6. Interfacial debonding length as a function of strain.

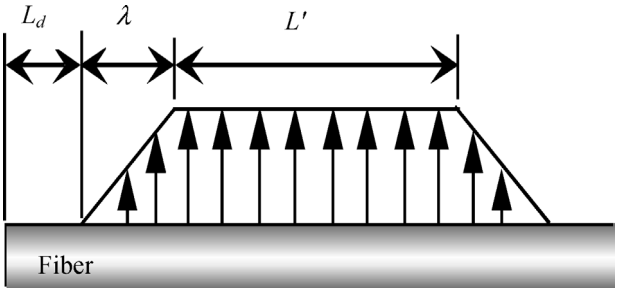

Figure 7. Tensile stress distribution of fiber.

we considered the effective fiber length, which is the length of the debonding length and the stress recovery length subtracted from the one-fragment fiber length as shown in Fig. 7. The test result of the number of fiber breaks that is considered to be an effective fiber length as a function of strain is shown in Fig. 8. The Weibull parameters were determined by the Weibull distribution of the fiber strength that closely matched the test results. In the test results, the relationship of the fiber strength and the fiber length is

$$E_f \varepsilon = 2500\left(\frac{25}{L}\right)^{1/13} \text{MPa}. \tag{21}$$

Thirdly, the interfacial shear stress is calculated from the state of the critical fragment. The fiber breakages become saturated due to the fact that as they are breaking, one fiber length is not long enough to recover the fiber strain that is identical to the specimen's strain. At this critical condition, all of the fibers have

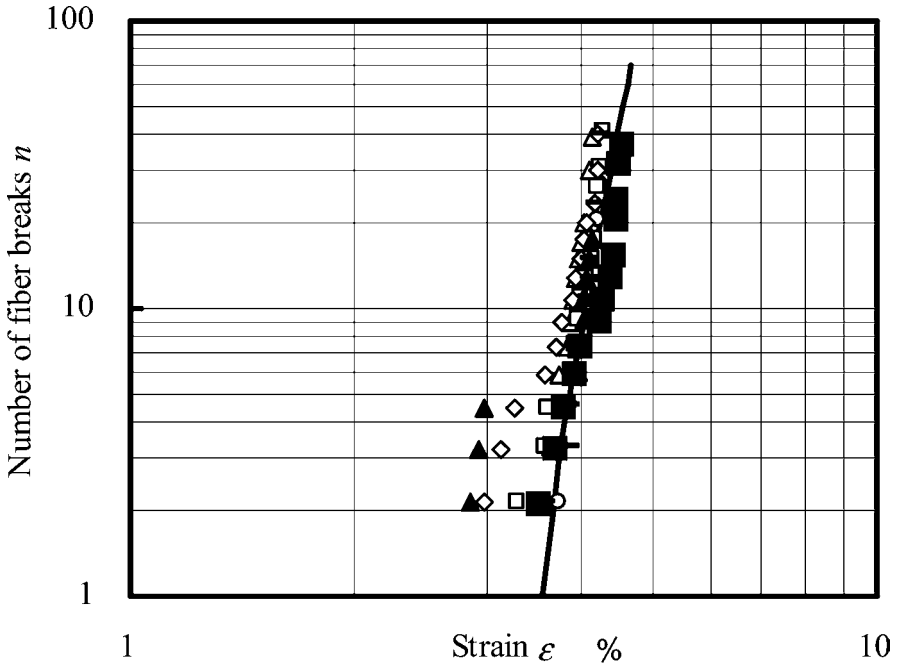

Figure 8. Number of fiber breaks as a function of strain.

only the stress recovery length and the interfacial debonding length; all fiber lengths are less than twice of the stress recovery length and the interfacial debonding length. And if the interfacial shear stress is assumed to be constant and the interfacial debonding does not exist, it can be estimated as follows based on Kelly-Tyson model [11].

$$\tau = \frac{3E_f \varepsilon D}{8\left(\dfrac{L_0}{n+1}\right)}. \tag{22}$$

Here n is the number of fiber breaks and L_0 is the measurement length. If we take into account the interfacial debonding length, the interfacial shear stress can be calculated as follows. Here we assume that the interfacial friction stress is neglected

$$\tau = \frac{3E_f \varepsilon D}{8\left(\dfrac{L_0}{n+1} - L_d\right)}. \tag{23}$$

The test results are indicated in Table 2. The value of the interfacial debonding length is applied in equation (20) above. So far, each static parameter that was used for the rupture model was determined, and it was possible to estimate the modified rupture strain of unidirectional glass fiber/vinylester composites in static loading conditions.

Table 2.
Critical properties of fragmentation test

Critical strain	ε_c	4.65%
Critical number of fiber breaks	n_c	33
Interfacial shear stress	τ	51 MPa

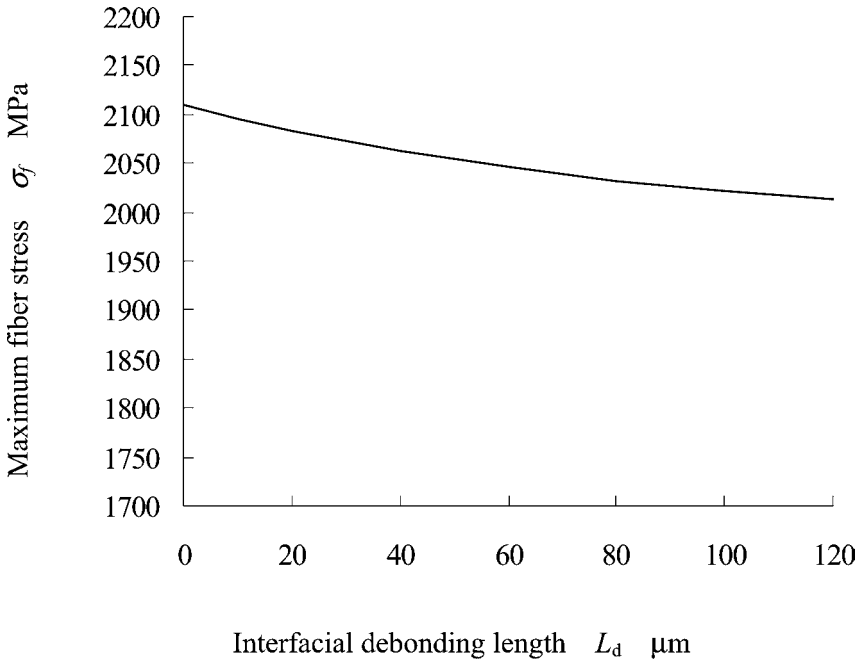

Figure 9. Maximum fiber stress as a function of interfacial debonding length.

4.2. Interfacial debonding propagation test

To ensure the long-term creep we must investigate the time-dependent failure. In long-term creep, macroscopically, the strain of a unidirectional composite would almost never increase; however, the interfacial debonding might grow. Figure 9 shows the relationship between the interfacial debonding length and the maximum fiber stress calculated by the modified Curtin model that takes into account the interfacial debonding length around the fiber breaks in unidirectional composites. As one can see from this figure, the interfacial debonding propagation causes the composite strength to be lowered. We performed the interfacial debonding propagation tests. The specimen was the same as that of the above fragmentation tests. After generating some fragment points, the interfacial debonding length was investigated in the condition in which the specimen was subjected to a constant strain because long-term creep should be assumed. As mentioned before, the composite strain would almost never increase in long-term creep because the matrix stress in the longitudinal direction would have relaxed completely. The test results

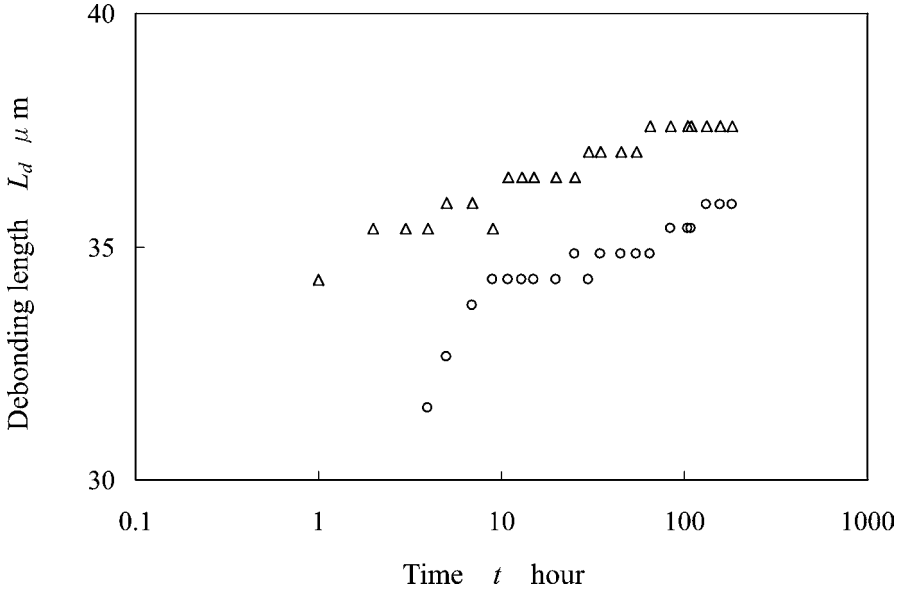

Figure 10. Results of interfacial debonding propagation tests.

are shown in Fig. 10. It is found that interfacial debonding grows under a constant strain as time progresses. In this study, the interfacial debonding length is evaluated as a function of time, and the relationship of the interfacial debonding length and log time is linear as follows.

$$L_d(t) = L_{d\text{int}} + 1.1 \times \log t. \tag{24}$$

4.3. Creep test

Creep tests were performed to investigate the two creep constants in the equation (2). We made unidirectional composite specimen consisting of a vinylester resin and a glass fiber bundle. The specimen dimensions were also the same as that of the specimen in the fragmentation test shown in Fig. 4. A fiber bundle substituting for the single fiber was embedded. The fiber volume fraction of this specimen was 2%.

Figure 11 displays the creep test results and theoretical curves. The two creep parameters are determined by the theoretical curve that matched with the test results. From these creep tests, the two creep constants of the vinylester matrix, $B = 2.5 \times 10^{-8}$/hour and $n = 2.2$, were determined.

5. PREDICTION OF CREEP RUPTURE AND DISCUSSION

The creep lifetime of glass fiber/vinylester unidirectional composites could be predicted with the use of the static and the time-dependent parameters as mentioned

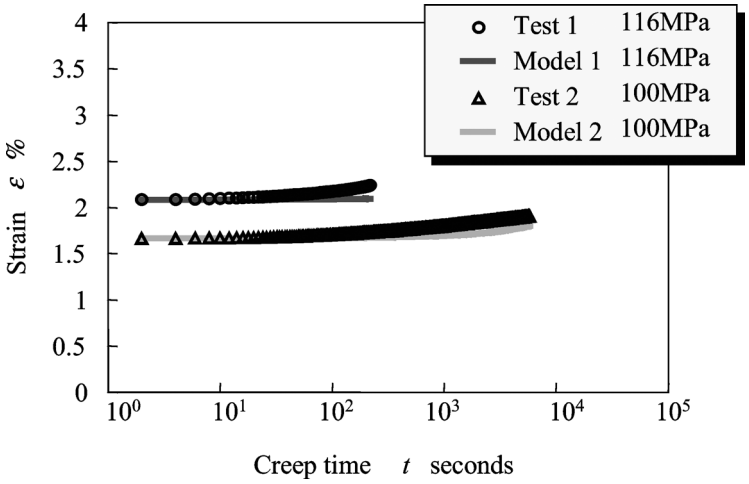

Figure 11. Creep behavior of unidirectional composite.

before. Figure 12 shows a creep time prediction of 2% volume fraction in unidirectional composite specimen. In this figure, the dotted line is the prediction of the creep rupture time based on the conventional model and the solid line is that based on the proposed model. The dotted symbols are the results of the creep rupture tests. In the range of this study, the difference between the two models was small because the interfacial debonding length was so short that it had no significant impact on the rupture strain. However, after a long while, the difference between the two models will become greater as predicted in Fig. 12. A threshold stress exists in the conventional model; on the other hand, there is no threshold stress in the proposed model because the interfacial debonding propagation lowers the rupture strain as time progresses. That is to say, we have to improve the creep model by taking interfacial debonding into account in the long-term creep.

The prediction of the creep rupture time in cases when the various debonding lengths were calculated by the modified model are shown in Fig. 13. The various interfacial-debonding propagation rates are assumed from hundred-times to ten thousand-times speed compared to the rate of the equation (24), which are the test results in this study. Figure 13 can predict that the faster the debonding rate, the more significantly it affects the creep lifetime. Therefore, we must perform the creep tests using the specimen whose interfacial properties are weak to verify the availability of this modified creep rupture model in the future works.

In this study, there is a reason that the test results and the theoretical line are in good agreement. The fiber volume fraction of these specimens was so low and the distance between fibers was so far that a stress concentration to neighboring fibers from the broken fibers was not effective. The model proposed in this study does not have a stress concentration factor. The typical fiber volume fraction of unidirectional composites is 50–70%, so it is natural that the adjacent fiber breaks occur. We will have to establish a new model that includes the stress

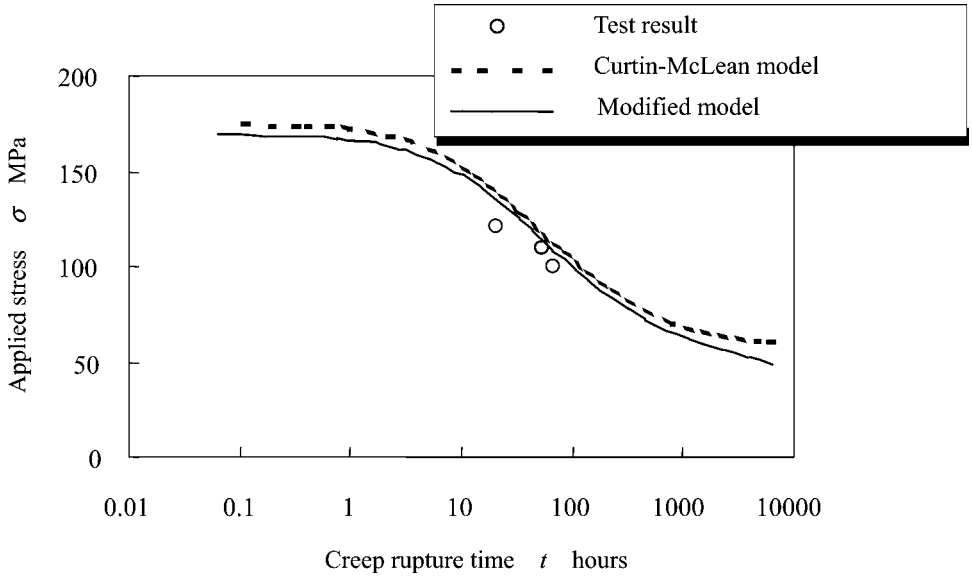

Figure 12. Prediction of creep life and experimental results.

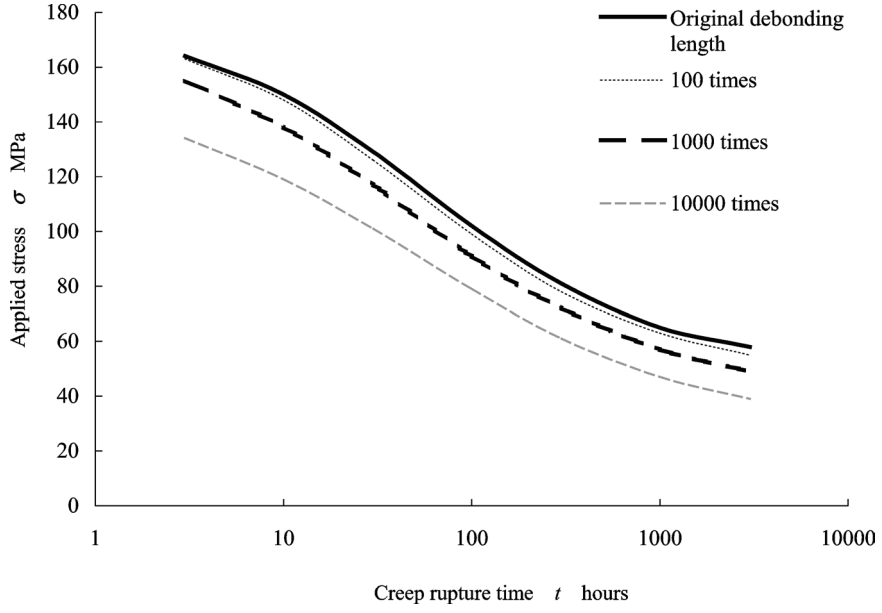

Figure 13. Prediction of creep life in various debonding length.

concentration factor and perform creep tests using the typical V_f specimen to verify the availability of such a model in the future works.

6. CONCLUDING REMARKS

In the fragmentation tests, it was found that the relationship between the fiber length and the probability of the fiber breaks was linear due to taking into account the effective fiber length.

The interfacial debonding causes the rupture strain in the unidirectional composite to decrease respectively. Therefore, in the case that the interfacial properties are relatively weak or that the interfacial debonding might grow in long-term creep, the proposed model must be applied for the creep rupture predictions.

There was no threshold stress in the proposed model because it had taken into account the fact that interfacial debonding propagation causes the rupture strain of unidirectional composites to decrease as time progresses.

REFERENCES

1. M. McLean, Creep deformation of metal-matrix composites, *Compos. Sci. Technol.* **23**, 37–52 (1985).
2. W. A. Curtin, Theory of mechanical properties of ceramic-matrix composites, *J. Amer. Ceramics Soc.* **74**, 2837–2845 (1991).
3. Z. Z. Du and R. M. McMeeking, Creep models for metal matrix composites with long brittle fibers, *J. Mechanics Physics Solids* **43**, 701–726 (1995).
4. P. Sofronis and R. M. McMeeking, The effect of interface diffusion and slip on the creep resistance of particulate composite materials, *Mechanics Materials* **18**, 55–68 (1994).
5. X. F. Zhou and H. D. Wagner, Fragmentation of two-fiber hybrid microcomposites: stress concentration factors and interfacial adhesion, *Compos. Sci. Technol.* **60**, 367–377 (2000).
6. N. Ohno, H. Kawabe, T. Miyake and M. Mizuno, A model for shear stress relaxation around fiber break in unidirectional composites and creep rupture analysis, *J. Soc. Mater. Sci. Japan* **47**, 184–191 (1998).
7. X. F. Zhou, J. A. Nairn and H. D. Wagner, Fiber–matrix adhesion from the single-fiber composite test: nucleation of interfacial debonding, *Composites Part A* **30**, 1387–1400 (1999).
8. X. F. Zhou, H. D. Wagner and S. R. Nutt, Interfacial properties of polymer composites measured by push-out and fragmentation tests, *Composites Part A* **32**, 1543–1551 (2001).
9. I. J. Beyerlein, C. H. Zhou and L. S. Schadler, A time dependent micro-mechanical fiber composite model for inelastic zone growth in viscoelastic matrices, *Intern. J. Solid Structure* **40**, 1–24 (2003).
10. I. J. Beyerlein and S. L. Phoenix, Time evolution of stress redistribution around multiple fiber breaks in a composite with viscous and viscoelastic matrices, *Intern. J. Solid Structure* **35**, 3177–3211 (1998).
11. D. Shia, C. Y. Hui and S. L. Phoenix, Statistics of fragmentation in a single-fiber composite under matrix yielding and debonding with application to the strength of multi-fiber composites, *Compos. Sci. Technol.* **60**, 2107–2128 (2000).